

18. BULK $\delta^{18}\text{O}$ AND $\delta^{13}\text{C}$ RECORDS FROM SITE 999, COLOMBIAN BASIN, AND SITE 1000, NICARAGUAN RISE (LATEST OLIGOCENE TO MIDDLE MIOCENE): DIAGENESIS, LINK TO SEDIMENT PARAMETERS, AND PALEOCEANOGRAPHY¹

Maria Mutti²

ABSTRACT

Stable isotope records spanning from the latest Oligocene through the middle Miocene have been produced at Sites 999 and 1000 to address major changes in climate associated with the transition from relative global warmth of the late Oligocene–early Miocene to the Neogene “ice-house” world.

The isotopic records of Sites 999 and 1000 clearly show the middle Miocene oxygen-isotope increase from ~15.5 to 13 Ma, and all Miocene oxygen-isotope events “Mi” can be recognized. Additional $\delta^{18}\text{O}$ increases occur at ~24.5, ~23, 20.5, and 17.8 Ma. In addition, the long-term $\delta^{18}\text{O}$ increase between ~15.5 and 13 Ma shows internal quasi-cyclic structures, reflecting a periodicity of ~400 k.y., the orbital eccentricity, which is superimposed on the longer term cooling trend related to the major ice-sheet growth in Antarctica. The long-term trends in carbon isotopes are marked by two positive excursions: the $\delta^{13}\text{C}$ increase near the Oligocene/Miocene boundary, from ~24.5 to 23 Ma, and the Monterey Excursion between ~17 and 13.5 Ma. The increase in $\delta^{13}\text{C}$ at 17 Ma leads the first major cooling step in Antarctica by 1.5 m.y. However, within the Monterey Excursion several $\delta^{13}\text{C}$ maxima occur with cyclic periods of ~400 k.y. in parallel to climate excursions as indicated by oxygen isotopes.

Long-term isotope shifts, coinciding with lithologic changes indicating the changes in sediment physical properties, are linked to changes in climate.

INTRODUCTION

One of the goals of Leg 165 was to sample deep-sea sediments to examine the nature of climate variability and changes in ocean circulation under a variety of boundary conditions present during the Cenozoic time. The late Oligocene–Miocene is a key interval in the global climatic evolution of the Cenozoic. The transition from relative global warmth of the late Oligocene–early Miocene to the Neogene “ice-house” world took place with a series of major changes in climate, polar ice volume, and ocean circulation. The middle Miocene $\delta^{18}\text{O}$ increase was a major step in this climate transition, reflecting a combination of Antarctic ice growth and deep-water cooling linked to circulation changes (Shackleton and Kennett, 1975; Woodruff et al., 1981; Miller et al., 1991; Woodruff and Savin, 1991; Wright et al., 1992). Paleooceanographic changes were accompanied by major variations in mean ocean $\delta^{13}\text{C}$, reflecting redistribution of carbon between reservoirs and changes in global carbon cycling (Vincent and Berger, 1985; Miller and Fairbanks, 1985; Kennett, 1986). Possible factors contributing to this climate transition include tectonic events that altered atmospheric and oceanic circulation, such as the opening and closing of major oceanic gateways (Kennett, 1982), or forcing factors that contributed to cooling via reduced greenhouse effect, such as the uplift of major orogenies that increased weathering (Raymo and Ruddiman, 1992; Raymo, 1994), and/or organic carbon burial rates (Vincent and Berger, 1985).

Stable isotope records spanning from the latest Oligocene through the middle Miocene were generated for Sites 999 and 1000, respectively (Fig. 1). This study has two major objectives. (1) Because stable isotope records from the Caribbean region are sparse for this time interval, it was considered useful to generate a record from these two

sites that can be compared with the chemostratigraphy already established from well-dated sections in other locations in the world. (2) To analyze over a time span of ~17 m.y. the detailed character of the carbon- and oxygen-isotope records and the relationships between these two climate proxies at this tropical location.

METHODS

Age Model

The age models for Sites 999 and 1000 are based on nannoplankton and planktonic foraminifer biostratigraphy (Sigurdsson, Leckie, Acton, et al., 1997; Kameo and Bralower, Chap. 1, this volume; Chaisson and D’Hondt, Chap. 2, this volume) and calibrated to the revised geomagnetic polarity time scale of Cande and Kent (1995). For comparison purposes, I have converted the ages of the Miocene $\delta^{18}\text{O}$ events from Miller et al. (1991) and Wright et al. (1992) and the $\delta^{13}\text{C}$ maxima from Woodruff and Savin (1991) to the same time scale (see Table 1).

Stable Isotopes

The investigated intervals of Sites 999 and 1000 are dominated by pelagic carbonate, which shows at both sites a differential degree of lithification, increasing with depth and ranging from oozes to limestones. To maintain consistency in the stable isotope record throughout the interval, bulk samples were analyzed. More than 350 samples were analyzed for stable isotope composition. Samples were dried at 60°C, then, according to their degree of lithification, either broken and crushed or drilled to obtain sufficient material for analysis. Then they were reacted using orthophosphoric acid at 90°C and analyzed online using a PRISM mass spectrometer at ETH Zurich. Results are reported using the standard δ notation in per million (‰) relative to the PDB standard. Reproducibility of replicate analyses was generally better than 0.1‰. The resolution of the stable isotope record is at an average of ~50 ka (up to ~35 ka) at Site 1000, and at an average of ~140 ka (ranging between 80 ka and 250 ka) at Site 999.

¹Leckie, R.M., Sigurdsson, H., Acton, G.D., and Draper, G. (Eds.), 2000. *Proc. ODP, Sci. Results*, 165: College Station, TX (Ocean Drilling Program).

²Department of Earth Sciences, University of Southern California, Los Angeles, CA 90089-0740, U.S.A. mmutti@earth.usc.edu (Present address: Institute of Geology and Paleontology, University of Stuttgart, Herdweg 51, D-70174 Stuttgart, Germany. maria.mutti@geologie.uni-stuttgart.de)

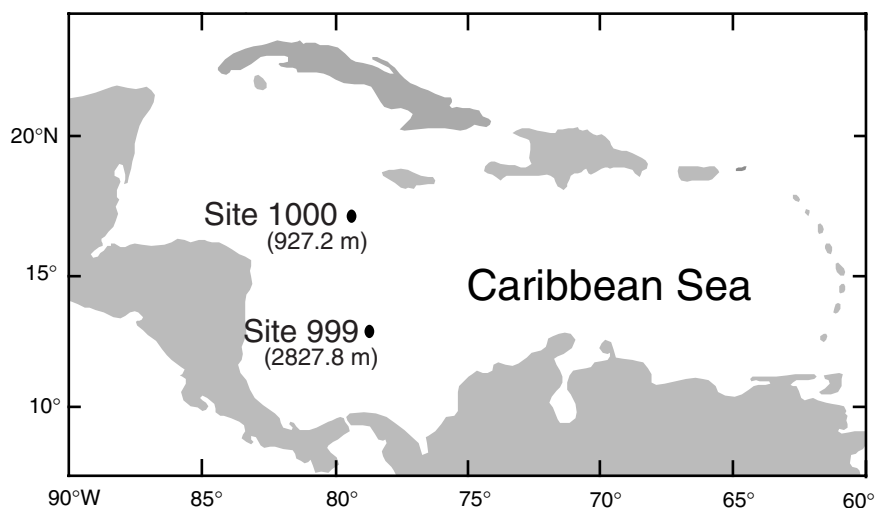


Figure 1. Location map of Sites 999 and 1000 in the Caribbean. M = mbsf.

Table 1. Conversion of Miocene oxygen- and carbon-isotope events from the geomagnetic polarity time scale to the time scale of Cande and Kent.

Event	Age* (Ma)	Age† (Ma)
Mi1	23.7	23.7
Mi1a	21.7	21.5
Mi1aa	20.0	19.7
Mi1b	18.3	18.0
Mi2	16.2	16.0
Mi3	13.6	13.6
Mi4	12.6	12.8
Mi5	11.3	11.7
CM1	16.4	16.2
CM2	15.8	16.1
CM3	15.5	15.4
CM4	15.1	15.0
CM5	14.5	14.4
CM6	14.1	14.1
CM7	11.5	11.9

Notes: * = Berggren et al. (1995); † = Cande and Kent (1995). The ages listed for the ^{18}O maxima are from Miller et al. (1991) and Wright et al. (1992); the age for the ^{13}C maxima (CM) are from Woodruff and Savin (1991).

Use of Bulk Isotopes

When comparing the data set generated at Sites 999 and 1000 with other existing records (e.g., Miller et al., 1998), a major difference to consider is that data generated in this study reflect bulk-rock analysis, rather than measurements on separate foraminiferal species. Bulk-rock analysis is uncommon in paleoceanographic and climate studies, which in most cases involve measurements on specific species of foraminifers. Even though bulk analyses reflect a mixing of carbonates from different sources, it has been shown that under certain circumstances, the isotopic composition derived from bulk analyses resembles closely the record derived from single foraminifer analyses (Shackleton and Hall, 1984; Shackleton et al., 1993). In some cases, bulk isotopes can be utilized when the lithologies are too lithified to allow separation of single foraminifers.

The isotopic composition of bulk samples is a function of the composition of the benthic and planktonic foraminifers and calcareous nannoplankton present, as well as their relative proportions. The $\delta^{18}\text{O}$ of foraminifers is a function of the seawater $\delta^{18}\text{O}$ value (δ_w) where the organism lived. Miocene oxygen-isotope events (Miller et al., 1991; Wright et al., 1992) reflect global changes, in δ_w , in both planktonic and benthic foraminifers, related to glacioeustatic fluctuations. In addition to glacioeustasy, changes in either temperature or salinity effect the $\delta^{18}\text{O}$ values.

BACKGROUND AND PREVIOUS WORK

Major paleoceanographic and climate changes that occurred during the middle Miocene represent a key step in the evolution of the Cenozoic. The middle Miocene $\delta^{18}\text{O}$ increase has been interpreted to primarily record the intensification of continental glaciation in Antarctica (Shackleton and Kennett, 1975; Savin et al., 1975; Savin and Woodruff, 1990; Woodruff et al., 1981). In this interpretation, cooling of high southern latitude surface waters increased the production of deep and intermediate waters and enhanced vertical stratification throughout the world ocean. Others have proposed a different interpretation in which large ice sheets may have existed prior to the middle Miocene and that the middle Miocene $\delta^{18}\text{O}$ increase was entirely caused by deep-water cooling, unaccompanied by Antarctic ice growth (Matthews and Poore, 1980; Prentice and Matthews, 1988). Drilling in the Ross Sea region of Antarctica (Barrett et al., 1987) confirmed the existence of intermittent continental ice sheets on Antarctica between the early Oligocene and the early Miocene. In addition, it remains controversial whether the middle Miocene step represented the development of a permanent ice sheet in East Antarctica (Matthews and Poore, 1980; Kennett and Barker, 1990). The relative proportions of $\delta^{18}\text{O}$ increase attributable to Antarctic ice storage or to bottom-water cooling remain uncertain.

Miocene climate changes may be related to changes in deep-water circulation. Several hypotheses have linked late Pliocene and Pleistocene climate changes (glacial/interglacial intervals) with changing fluxes of North Atlantic Deep Water (NADW) (e.g., Shackleton et al., 1993). The middle Miocene $\delta^{18}\text{O}$ increase has been linked to changes in Northern Component Water (NCW) (Schnitker, 1980) or Tethyan water (Woodruff and Savin, 1989). However, there is still much discussion regarding circulation patterns of deep water during the Miocene (see summary in Wright et al., 1992). Planktonic-benthic foraminiferal $\delta^{18}\text{O}$ covariance at low latitudes associated with major oxygen-isotope events (Miller et al., 1991; Wright and Miller, 1993) suggests that Antarctic ice sheets waxed and waned throughout the early and middle Miocene. More recently, Zachos et al. (1997) have shown a strong 40 ka periodicity in an equatorial oxygen-isotope record, consistent with a high-latitude orbital control on ice volume and temperature.

Miocene paleoceanographic changes were accompanied by major variations in mean ocean $\delta^{13}\text{C}$, involving redistribution between carbon reservoirs (Vincent and Berger, 1985; Miller and Fairbanks, 1985; Kennett, 1986). The mean $^{13}\text{C}/^{12}\text{C}$ ratio is generally controlled by the proportions of carbon deposited as organic carbon vs. calcium carbonate in the deep sea. Assuming that the rate of delivery to the ocean of terrestrial organic carbon, depleted in $\delta^{13}\text{C}$, did not vary

greatly during the Cenozoic, a higher mean $^{13}\text{C}/^{12}\text{C}$ ratio reflects an increase in organic carbon storage (e.g., Vincent and Berger, 1985). Two major maxima in mean ocean $\delta^{13}\text{C}$ occurred during the late Oligocene–Miocene: the first near the Oligocene/Miocene boundary, ~24 Ma (Zachos et al., 1997), and the second during the late early to middle Miocene from 17 to 13.5 Ma, termed the Monterey Carbon Isotope Excursion (Vincent and Berger, 1985). The Monterey $\delta^{13}\text{C}$ maximum has been attributed to the storage of large volumes of organic carbon in the Monterey Formation of California, circum-North Pacific, and the southeastern shelf of the United States, and it is postulated as a major contributor to global cooling through drawdown of atmospheric CO_2 and a series of positive-feedback mechanisms (Vincent and Berger, 1985). Although a time lag between the inception of the Monterey Formation deposition at 17.85 ± 0.1 Ma (DePaolo and Finger, 1991) and major global cooling at 14.8–14.0 Ma represents a difficulty with this hypothesis, it has been proposed that episodic increases in organic carbon burial within the Monterey Formation may have contributed to accelerated atmospheric drawdown of CO_2 and global cooling (Flower and Kennett, 1993a, 1993b). Strong covariance between deep-sea $\delta^{18}\text{O}$ and $\delta^{13}\text{C}$ records from 16 to 13.5 Ma (Woodruff and Savin, 1991) and the $\delta^{18}\text{O}$ correlation between the Monterey Formation at Naples Beach and the deep-sea record from 14.5 to 14.1 Ma (Flower and Kennett, 1993a) suggest a linkage between organic carbon burial, deep-water cooling, and ice-volume changes.

LITHOSTRATIGRAPHIC UNITS

Site 999

Site 999 is on the Kogi Rise, located ~1000 m above the turbidite-laden floor of the Colombian Basin (Fig. 1). A 1066-m-thick continuous and apparently complete upper Maastrichtian–Pleistocene section was recovered. This section consists dominantly of pelagic sedi-

ments and sedimentary rocks with variable amounts of clays and volcanic ash (Fig. 2). The investigated interval at Site 999 ranges from 250 to 640 mbsf, spanning from the upper Oligocene through the base of the upper Miocene (Fig. 2). This interval comprises different lithostratigraphic units (Units II, III, and IV) (see Fig. 2) determined on board ship on the basis of sedimentologic criteria, magnetic susceptibility, color reflectance, and carbonate content (Sigurdsson, Leckie, Acton, et al., 1997).

Site 1000

Site 1000 is located in Pedro Channel, one of a series of channels that dissects the carbonate banks defining the Nicaraguan Rise (Fig. 1). A continuous, fairly homogeneous lower Miocene to Holocene section (696 m thick) was recovered, which consists dominantly of periplatform sediments and sedimentary rocks, interbedded with volcanic ash layers and intervals of redeposited pelagic and neritic carbonates from the adjacent shallow carbonate banks (Fig. 3). The interval spanning from the lower Miocene through the base of the upper Miocene (Fig. 3), ranging from 300 to 696 mbsf (the bottom of the recovered section), comprises different lithostratigraphic subunits (Subunits IC, ID, IIA, and IIB) (see Fig. 3) determined on board ship on the basis of sedimentologic criteria, magnetic susceptibility, color reflectance, and carbonate content (Sigurdsson, Leckie, Acton, et al., 1997). The investigated interval at Site 1000 ranges from 370 to 696 mbsf.

RESULTS

Site 999

The oxygen-isotope record shows marked variations, ranging from -2.77‰ to -0.28‰ (Fig. 4). Oxygen-isotope values show three major features: (1) an irregular but consistent increase from -2.64‰

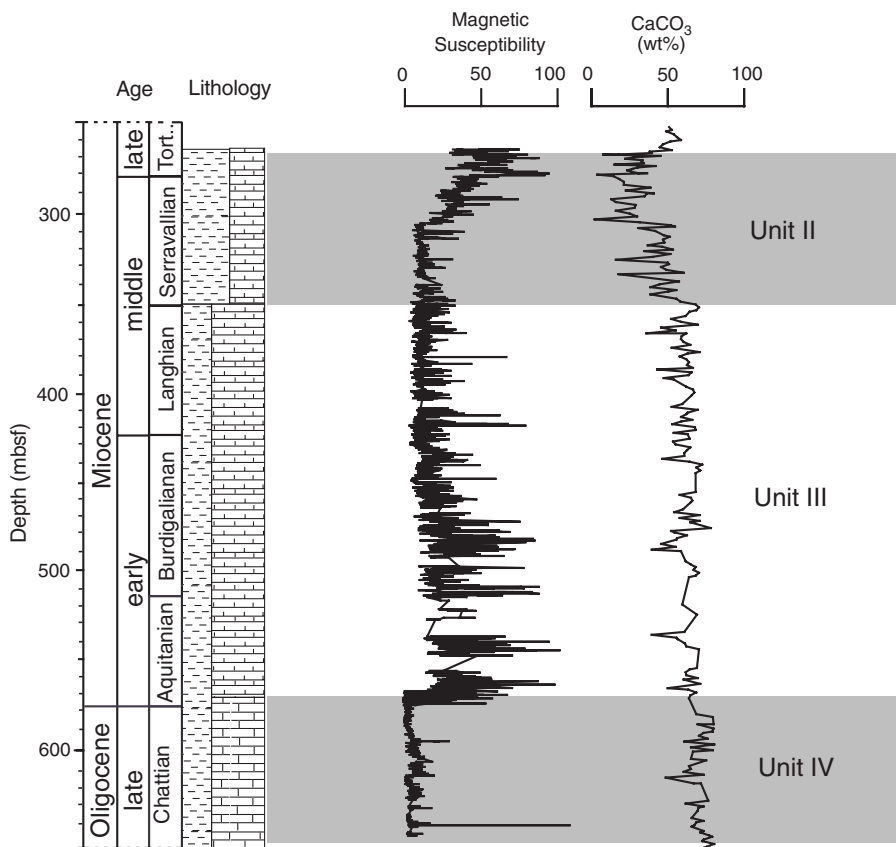


Figure 2. Lithostratigraphic units in the investigated interval at Site 999 (Subunits IC, IIA, and IIB, Unit III, and Subunit IVA) primarily reflect changes in magnetic susceptibility, carbonate content, and degree of lithification. Note that ash layers have been removed from magnetic susceptibility data so that it reflects only background sedimentation.

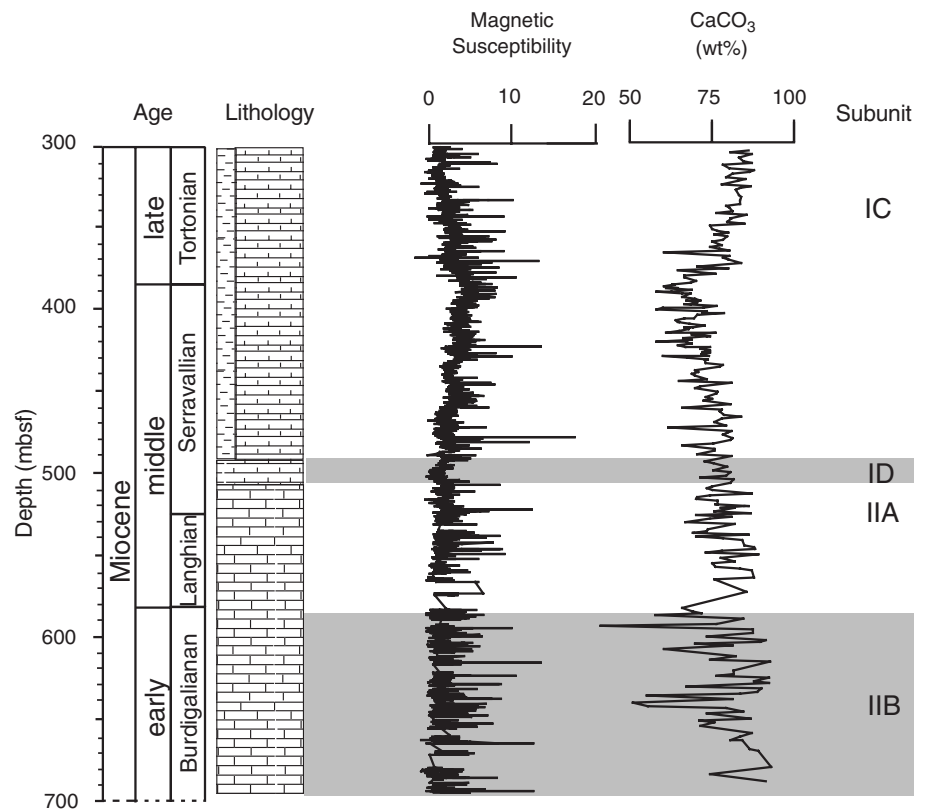


Figure 3. Lithostratigraphic subunits in the investigated interval at Site 1000 (Subunits IC, ID, IIA, and IIB) primarily reflect changes in magnetic susceptibility, carbonate content, and degree of lithification. Magnetic susceptibility data reflects only background sedimentation, as ash layers have been removed.

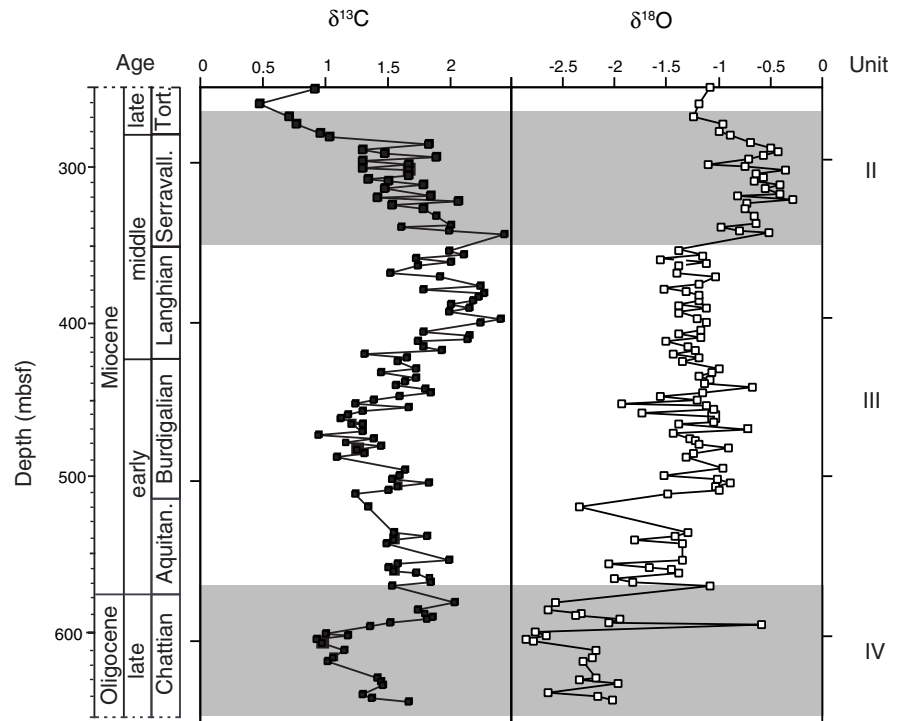


Figure 4. Carbon- and oxygen-isotope data from Site 999. Gray and white intervals correspond to lithostratigraphic units, as shown in Figure 2.

to -1.30‰ , spanning across lithostratigraphic Unit IV and the lower part of Unit III, from the Chattian through the Aquitanian stages, (2) a phase of relatively constant values throughout the Burdigalian and Langhian stages, and (3) an abrupt increase at the boundary between lithostratigraphic Units III and II, from -1.30 to -0.52 . These distinctive patterns in oxygen isotopes match lithostratigraphic Units II, III, and IV (see Fig. 4), raising the question on whether the oxygen-

isotope values reflect in part diagenetic alteration. The bulk oxygen-isotope values at this site, comprised between -2.8‰ and -0.5‰ , can be subdivided into two zones: a lower zone (510–650 mbsf) characterized by a large variability of $\delta^{18}\text{O}$ values ranging from -2.8‰ to -0.5‰ , and an upper zone (250–510 mbsf) characterized by a minor variability of $\delta^{18}\text{O}$ from -2‰ to -0.5‰ . Values comprised between -2.2‰ and -0.5‰ are typical values for planktonic organisms, sug-

gesting that the $\delta^{18}\text{O}$ values of the upper zone primarily reflect the isotopic composition of planktonic foraminifers and nannoplankton.

Burial depth as well as CaCO_3 content are useful proxies to evaluate the extent of diagenetic modification to oxygen-isotope values. Frank et al. (1998) have shown that with increasing CaCO_3 content and burial depth, bulk-rock values become progressively more depleted in $\delta^{18}\text{O}$. In order to evaluate the effect of diagenesis, oxygen-isotope values have been plotted against percentages of CaCO_3 (Fig. 5). Although, generally speaking, the samples from the lower zone at Site 999, characterized by the lower $\delta^{18}\text{O}$ values, coincide with high CaCO_3 content, there is not an unambiguous correlation between the two parameters (Fig. 5). The boundary between lithostratigraphic Units IV and III is found within the zone of light $\delta^{18}\text{O}$ values; below this stratigraphic boundary, the correlation between lower $\delta^{18}\text{O}$ values and high CaCO_3 seems more consistent.

This correlation would suggest that the $\delta^{18}\text{O}$ values might have been altered as a consequence of postdepositional precipitation of CaCO_3 in the pores, causing a modification to the depositional marine values when analyzed as bulk samples. However, these samples contain a large number of planktonic foraminifers, naturally characterized by lower $\delta^{18}\text{O}$ values than benthic foraminifers. The correlation between $\delta^{18}\text{O}$ and CaCO_3 content is reverted in Unit II, changing exactly at the boundary. At this shallow burial depth (<350 mbsf), no diagenetic modification to the $\delta^{18}\text{O}$ is expected, suggesting that there is a primary, depositional relationship between isotopic values and lithostratigraphic units.

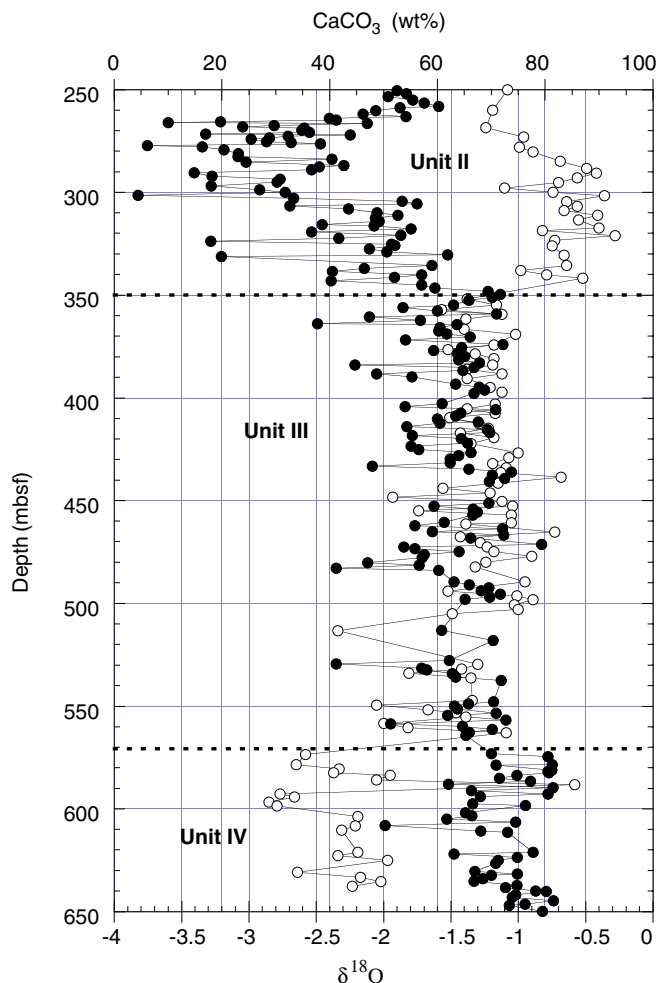


Figure 5. Oxygen-isotope data from Site 999 (this study) plotted against carbonate content (Sigurdsson, Leckie, Acton, et al., 1997). Solid symbols indicate carbonate data, open symbols indicate oxygen-isotope data.

In summary, the $\delta^{18}\text{O}$ values from the upper zone seem to have been unaffected by burial diagenesis, and therefore reflect primary values. The values for the lower zone, particularly from Unit IV have possibly been affected by burial diagenesis, which resulted in a depletion of the $\delta^{18}\text{O}$ values and must therefore be treated with caution when analyzed for paleoceanographic purposes.

The carbon-isotope record shows marked variations, from 0.47‰ to 2.44‰, and two major positive excursions can be recognized (Fig. 4). The first $\delta^{13}\text{C}$ shift is in the upper Oligocene within lithostratigraphic Unit IV and is a fairly abrupt increase from 0.92‰ to 2.03‰ found within ~23 m of sediment thickness. This shift shows a gradual and steplike return to lower values during the Aquitanian. The second $\delta^{13}\text{C}$ shift is in the upper lower Miocene within lithostratigraphic Unit III and is a gradual, stepwise increase over a thicker interval than the upper Oligocene increase initiated during the Burdigalian, from 0.94‰ to 1.84‰, returning to 1.31‰ and then rapidly increasing to 2.40‰ during the Langhian. The carbon values remain high for ~40 m and then start gradually returning to lower values throughout the Serravallian. The excursion terminates with a gradual but rapid return to 0.95‰ at the end of the Serravallian.

Site 1000

With respect to Site 999, the carbon- and oxygen-isotope data obtained from Site 1000 are characterized by higher time resolution, with an average of ~50 ka (Fig. 6). For clarity of data presentation, carbon- and oxygen-isotope data have been smoothed using a 5-point running average (Fig. 7).

The oxygen-isotope record (Figs. 6, 7) shows marked variations, ranging from -2.74‰ to -0.30‰, with a systematic trend toward heavier values upsection and the detailed character of lower and middle Miocene shifts. There are three first-order features that can be recognized in comparison with the record from Site 999: (1) an interval with high variability but without a marked trend during the Burdigalian, (2) a phase of progressive shift toward heavier values, from -2.34‰ to -0.93‰, peaking at -0.30‰, and (3) relatively constant values during the Serravallian with values ranging from -1.7‰ to -0.6‰. Compared to data from Site 999, the higher resolution $\delta^{18}\text{O}$ data at Site 1000 show in more detail the structure of the middle Miocene $\delta^{18}\text{O}$ increase; this, totaling 1.4‰, is found within several (three to four) quasi-cyclic steps.

Similar to Site 999, distinctive patterns in oxygen isotopes correspond to different lithostratigraphic subunits (Subunits IIB, IIA, ID, and IC) (see Fig. 3), raising the question on whether the oxygen-isotope values reflect, in part, diagenetic alteration. In order to evaluate the effect of diagenesis, especially in the deeper part of the record (590–696 mbsf), isotope values have been plotted against percentages of CaCO_3 (Fig. 8). At this site, in Subunit IIB, the highest variability of oxygen values corresponds to the highest variability in CaCO_3 values, suggesting that these values might have been altered.

The carbon-isotope record shows marked variations, from 0.52‰ to 2.18‰, and one major positive excursion can be recognized (Fig. 7). The positive $\delta^{13}\text{C}$ shift is a stepwise increase, initiated during the Burdigalian, with a gradual increase from 0.94‰ to 1.46‰, then rapidly increasing to 2.18‰ at the end of the Burdigalian, remaining high during the Langhian and reaching highest values in the early Serravallian. The $\delta^{13}\text{C}$ values start gradually returning to lower values throughout the Serravallian, reaching 0.7‰. Toward the end of the Serravallian there is a shift to higher values (up to 1.62‰), followed by an abrupt decrease from 1.62‰ to 0.61‰ at the end of the Serravallian.

DISCUSSION

Oxygen Isotopic Records

The marked variations in oxygen isotopes recognized in the records of Sites 999 and 1000 can be traced between the two sites, al-

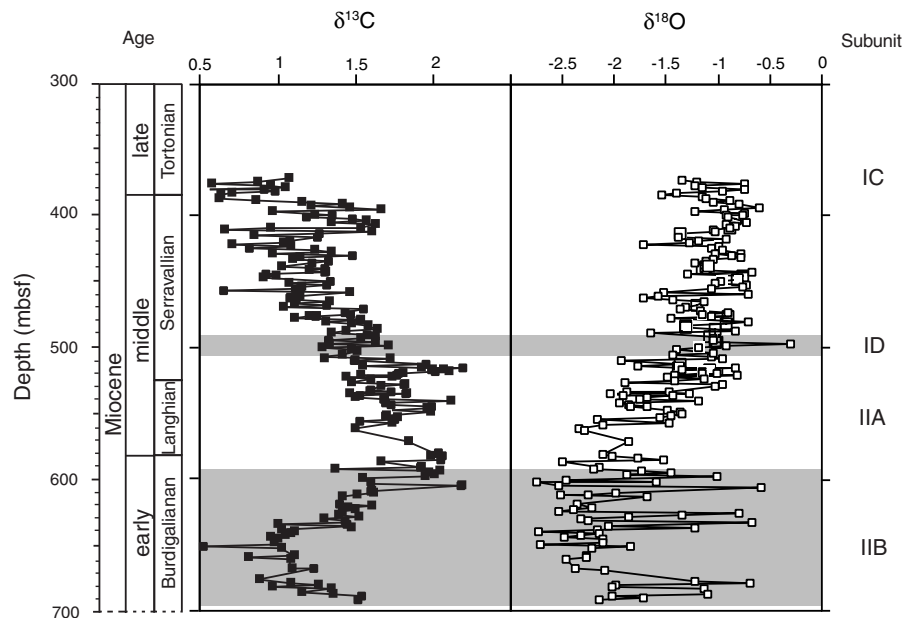


Figure 6. Carbon- and oxygen-isotope data from Site 1000. Gray and white intervals correspond to lithostratigraphic subunits, as shown in Figure 3.

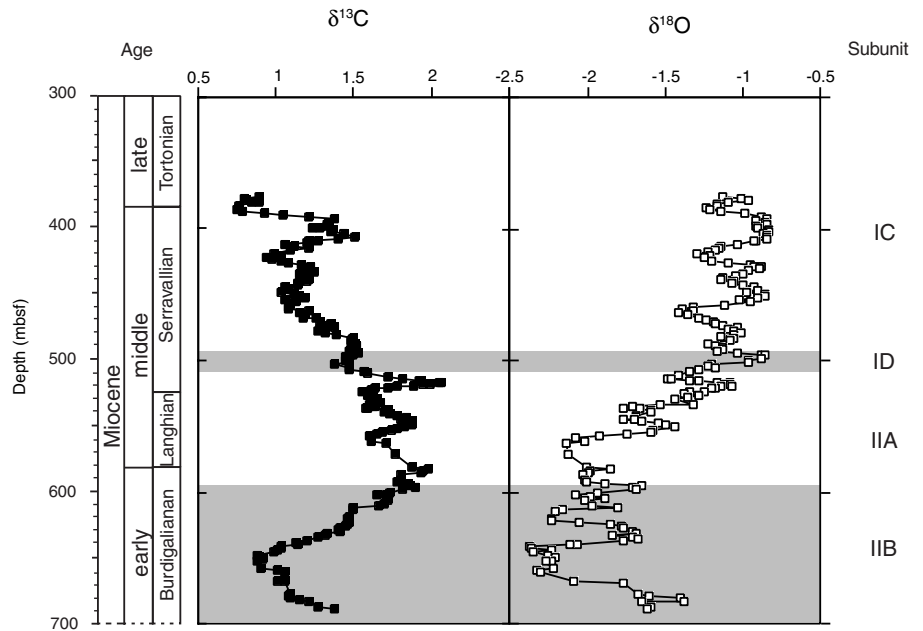


Figure 7. Carbon- and oxygen-isotope data from Site 1000 smoothed by a 5-running average. Note that this removes periods shorter than ~300 k.y. Gray and white intervals correspond to lithostratigraphic subunits, as shown in Figure 3.

though they show a different temporal resolution. Both Sites 999 and 1000 record clearly the middle Miocene $\delta^{18}\text{O}$ increase from ~15.5 to 13 Ma (Fig. 9).

A number of features emerge from a comparison of the $\delta^{18}\text{O}$ record from Sites 999 and 1000 with globally recognized Miocene oxygen-isotope events (as defined by Miller et al., 1991; Wright et al., 1992; Miller, Mountain, et al., 1996, 1998; Abreu and Haddad, in press). At Site 1000, the $\delta^{18}\text{O}$ record contains the Miocene oxygen-isotope events Mi2, Mi3, Mi4, and Mi5 (as defined by Miller et al., 1991; Wright et al., 1992). At Site 999, in addition to the events seen at Site 1000, the oxygen-isotope record also contains events Mi1, Mi1a, and Mi1aa.

One of the more interesting features of this record is that at Site 1000 the long-term $\delta^{18}\text{O}$ increase between ~15.5 and 13 Ma shows superimposed internal quasi-cyclic structures, which appears to reflect a periodicity of 400 k.y. or 1 m.y., as described by Miller et al. (1998), reflecting the orbital eccentricity.

Because the sites are located in the tropical ocean, variations in sea-surface temperature are expected to be minor and are, therefore, unlikely to cause the observed long-term trend of ~1.4‰ between ~15.5 and 13 Ma, which is interpreted to reflect mainly changes in Antarctic ice volume.

Carbon Isotopic Records

The marked variations in ^{13}C recognized in the Site 999 and 1000 records can be clearly correlated between the two sites (Fig. 10). The two most prominent features include the $\delta^{13}\text{C}$ increase near the Oligocene/Miocene boundary (see Zachos et al., 1997), observable at Site 999, from ~24.5 to 23 Ma, and, observable at both sites, the well-known interval of high $\delta^{13}\text{C}$ values between ~17 and 13.5 Ma (the Monterey Excursion) (Vincent and Berger, 1985). In addition, the $\delta^{13}\text{C}$ record from Sites 999 and 1000 shows all of the seven $\delta^{13}\text{C}$ maxima (CM1 through CM6) (Woodruff and Savin, 1991; Flower and

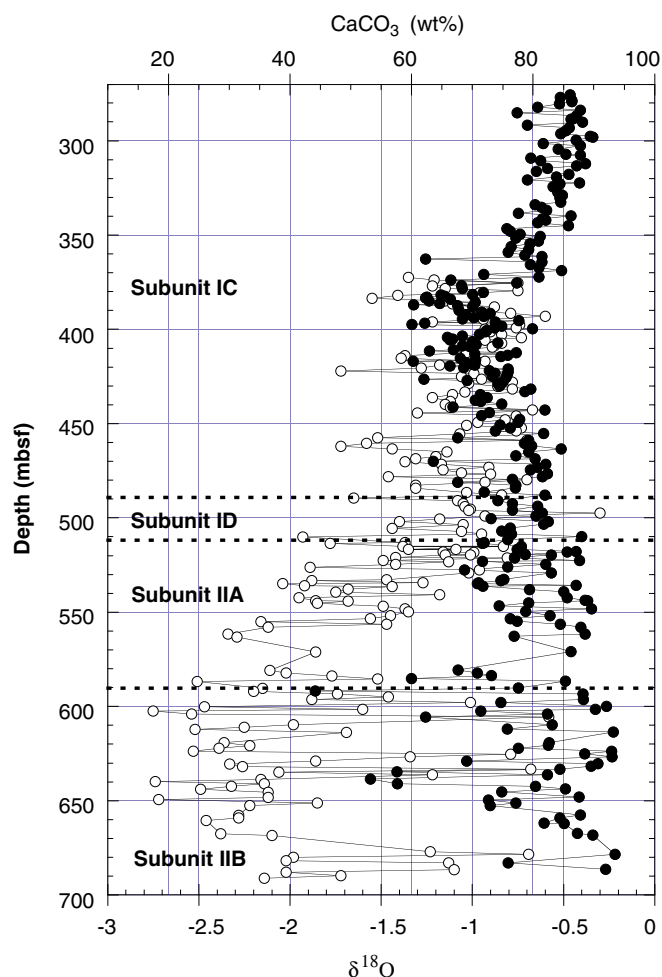


Figure 8. Oxygen-isotope data from Site 1000 (this study) plotted against carbonate content (Sigurdsson, Leckie, Acton, et al., 1997). Solid symbols indicate carbonate data, open symbols indicate oxygen-isotope data.

Kennett, 1993b) found within the Monterey Carbon Isotopic Excursion. The $\delta^{13}\text{C}$ maxima occur with quasi-cyclic periods of ~ 400 k.y.

The Miocene was a time of unusually high accumulation of organic matter around the Pacific, Atlantic, and Mediterranean (e.g., Monterey Formation, California: Vincent and Berger, 1985; Ingle, 1981; Florida shelf: Compton et al., 1990; Tellaro Formation, Sicily: Mutti et al., in press). Woodruff and Savin (1991) suggested that the seven $\delta^{13}\text{C}$ maxima found within the Monterey Carbon Isotopic Excursion correspond to episodes of accumulation of especially large amounts of organic matter around the world. The enhanced burial of organic matter during intervals of high $\delta^{13}\text{C}$ values may have been a major factor in reducing atmospheric CO_2 levels. This is further suggested by the association of $\delta^{13}\text{C}$ maxima with the $\delta^{18}\text{O}$ maxima (Woodruff and Savin, 1991) at Sites 999 and 1000.

Relationship between Oxygen and Carbon Isotopic Records

The data from this study confirm that the increase in carbon-isotope values at 17 Ma leads the first major cooling step in Antarctica at ~ 15.5 Ma (e.g., Vincent and Berger, 1985; DePaolo and Finger, 1991). Even though the first trend toward increased $\delta^{13}\text{C}$ values is associated with an immediate response in oxygen isotopes at Site 1000, suggesting modest changes in ice volume, an additional 1.5 m.y. is needed until full development of the Monterey Formation is

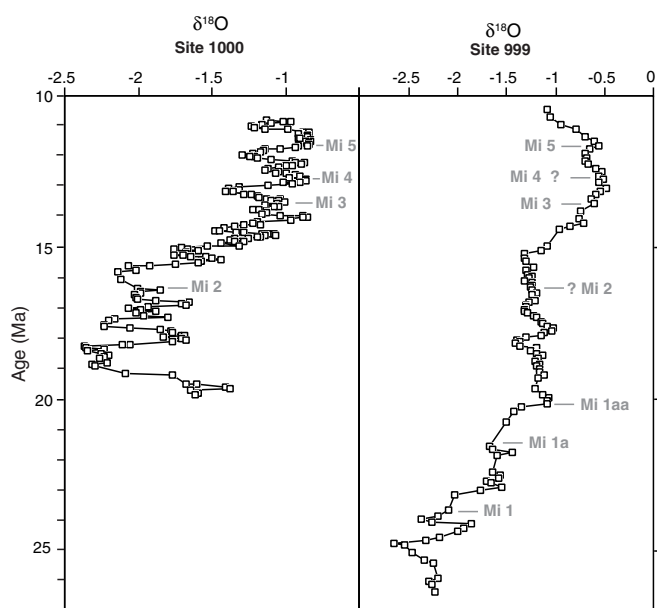


Figure 9. Oxygen-isotope data for Sites 1000 and 999 plotted against age. The chronologies at both sites remain based on biostratigraphy. The short horizontal gray lines indicate Miocene ^{18}O maxima from Miller et al. (1991) and Wright et al. (1993).

reached and major ice-sheet growth in Antarctica is evident as indicated by the oxygen- and carbon-isotope records of Sites 999 and 1000, and as also described elsewhere (Wright et al., 1991; Woodruff and Savin, 1991). During this major intensification of ice-sheet growth between ~ 15.5 and 14.5 Ma, the quasi-cyclic waxing and waning of Antarctica ice sheets is paralleled by positive excursions in carbon isotopes.

CONCLUSIONS

Variations in stable isotopes from Sites 999 and 1000 are linked to major changes in climate associated with the transition from relative global warmth of the late Oligocene–early Miocene to the Neogene “ice-house” world.

The oxygen-isotope increase between ~ 15.5 and 14.5 Ma is related to the major ice-sheet growth in Antarctica. This major climatic transition is characterized by a quasi-cyclic internal structure of ~ 400 k.y. reflecting variations in orbital eccentricity. This points to orbitally driven waxing and waning of Antarctica ice sheets.

The long-term trends in carbon isotopes are marked by two positive excursions: the $\delta^{13}\text{C}$ increase near the Oligocene/Miocene boundary, from ~ 24.5 to 23 Ma, and the Monterey Excursion between ~ 17 and 13.5 Ma. In addition, within the Monterey Excursion, several $\delta^{13}\text{C}$ maxima occur with quasi-cyclic periods of ~ 400 k.y.

The increase in $\delta^{13}\text{C}$ at 17 Ma leads the first major cooling step in Antarctica by 1.5 m.y. However, all short-term climate excursions as indicated by oxygen isotopes seem to be linked to shorter term $\delta^{13}\text{C}$ maxima.

ACKNOWLEDGMENTS

The author thanks ODP for providing the samples for this study and acknowledges the financial support of the Swiss National Science Foundation to participate in Leg 165. Funding for the analytical costs for stable isotope analyses were provided by the Swiss National Science Foundation. The technical support of the Stable Isotope Lab-

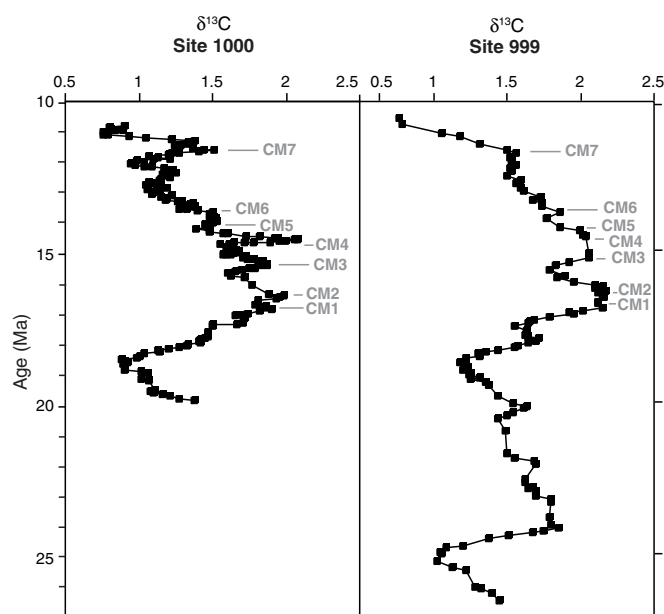


Figure 10. Carbon-isotope data for Sites 1000 and 999 plotted against age. The chronologies at both sites remain based on biostratigraphy. The short horizontal gray lines indicate the Miocene ^{13}C maxima (CM) from Woodruff and Savin (1991).

oratory in Zurich is gratefully acknowledged. Jane Teranes and Miriam Andres are thanked for their help in processing the samples. The manuscript benefited from the careful reviews by Ben Flower, Evan Franseen, and Mark Leckie.

REFERENCES

- Abreu, V.S., and Haddad, G.A., in press. Glacioeustatic fluctuations: the mechanism linking stable isotope events and sequence stratigraphy from the early Oligocene to middle Miocene. *Spec. Publ.—Soc. Econ. Paleontol. Mineral.*, 60.
- Barrett, P.J., Elston, D.P., Harwood, D.M., McKelvey, B.C., and Webb, P.N., 1987. Mid-Cenozoic record of glaciation and sea level change on the margin of the Victoria Land basin, Antarctica. *Geology*, 15:634–637.
- Berggren, W.A., Kent, D.V., Swisher, C.C., III, and Aubry, M.-P., 1995. A revised Cenozoic geochronology and chronostratigraphy. In Berggren, (Eds.), *Geochronology, Time Scales and Global Stratigraphic Correlation*. Spec. Pub.—Soc. Econ. Paleontol. Mineral. (Soc. Sediment. Geol.), 54:129–212.
- Cande, S.C., and Kent, D.V., 1995. Revised calibration of the geomagnetic polarity timescale for the Late Cretaceous and Cenozoic. *J. Geophys. Res.*, 100:6093–6095.
- Compton, J.S., Snyder, S.W., and Hodell, D.A., 1990. Phosphogenesis and weathering of shelf sediments from the Southeastern United States: Implications for Miocene $\delta^{13}\text{C}$ excursions and global cooling. *Geology*, 18:1227–1230.
- DePaolo, D.J., and Finger, K.L., 1991. High-resolution strontium-isotope stratigraphy and biostratigraphy of the Miocene Monterey Formation, central California. *Geol. Soc. Am. Bull.*, 103:112–124.
- Flower, B.P., and Kennett, J.P., 1993a. Middle Miocene ocean/climate transition: high-resolution oxygen and carbon isotopic records from DSDP Site 588A, Southwest Pacific. *Paleoceanography*, 8:811–843.
- , 1993b. Relations between Monterey formation deposition and middle Miocene global cooling: Naples Beach section, California. *Geology*, 21:877–880.
- Frank, T.D., Arthur, M.A., and Dean, W.E., 1998. Interpreting geochemical signals in pelagic carbonates: controls on diagenetic signatures. *GSA Ann. Meeting*, 55.
- Ingle, J.C., Jr., 1981. Origin of Neogene diatomites around the north Pacific rim. In Garrison, R.E., Douglas, R., Pisciotto, K., Isaacs, C., and Ingle, J.C. (Eds.), *The Monterey Formation and Related Siliceous Rocks of California*. Spec. Publ.—Soc. Econ. Paleontol. Mineral., 15:159–179.
- Kennett, J.P., 1982. Cenozoic Evolution of Antarctic glaciation, the circum-Antarctic ocean, and their impact on global paleoceanography. *J. Geophys. Res.*, 82:3843–3859.
- , 1986. Miocene to early Pliocene oxygen and carbon isotope stratigraphy in the southwest Pacific, Deep Sea Drilling Project Leg 90. In Kennett, J.P., von der Borch, C.C., et al., *Init. Repts. DSDP*, 90 (Pt. 2): Washington (U.S. Govt. Printing Office), 1383–1411.
- Kennett, J.P., and Barker, P.F., 1990. Latest Cretaceous to Cenozoic climate and oceanographic developments in the Weddell Sea, Antarctica: an ocean-drilling perspective. In Barker, P.F., Kennett, J.P., et al., *Proc. ODP, Sci. Results*, 113: College Station, TX (Ocean Drilling Program), 937–960.
- Matthews, R.K., and Poore, R.Z., 1980. Tertiary $\delta^{18}\text{O}$ record and glacio-eustatic sea-level fluctuations. *Geology*, 8:501–504.
- Miller, K.G., and Fairbanks, R.G., 1985. Evidence for Oligocene-middle Miocene abyssal circulation changes in the western North Atlantic. *Nature*, 306:250–253.
- Miller, K.G., Mountain, G.S., Browning, J.V., Kominz, M., Sugarman, P.J., Christie-Blick, N., Katz, M., and Wright, J.D., 1998. Cenozoic global sealevel, sequences, and the New Jersey transect: results from coastal plain and continental slope drilling. *Rev. Geophys.*, 36:569–601.
- Miller, K.G., Mountain, G.S., the Leg 150 Shipboard Party and Members of the New Jersey Coastal Plain Drilling Project, 1996. Drilling and dating New Jersey Oligocene–Miocene sequences: ice volume, global sea level and Exxon records. *Science*, 271:1092–1095.
- Miller, K.G., Wright, J.D., and Fairbanks, R.G., 1991. Unlocking the Ice House: Oligocene–Miocene oxygen isotopes, eustasy, and margin erosion. *J. Geophys. Res.*, 96:6829–6848.
- Mutti, M., Bernoulli, D., Spezzaferri, S., and Stille, P., in press. Lower and Middle Miocene carbonate facies in the Central Mediterranean: the impact of paleoceanography on sequence stratigraphy. In Harris, P.M., et al. (Eds.), *Advances in Carbonate Sequence Stratigraphy: Application to Reservoirs, Outcrops and Models*. Spec. Publ.—Soc. Econ. Paleontol. Mineral., 64.
- Prentice, M.L., and Matthews, R.K., 1988. Cenozoic ice-volume history: development of a composite oxygen isotope record. *Geology*, 16:963–966.
- Raymo, M.E., 1994. The Himalayas, organic carbon burial, and climate in the Miocene. *Paleoceanography*, 9:399–404.
- Raymo, M.E., and Ruddiman, W.F., 1992. Tectonic forcing of late Cenozoic climate. *Nature*, 359:117–122.
- Savin, S.M., Douglas, R.G., and Stehli, F.G., 1975. Tertiary marine paleotemperatures. *Geol. Soc. Am. Bull.*, 86:1499–1510.
- Savin, S.M., and Woodruff, F., 1990. Isotopic evidence for temperature and productivity in the Tertiary oceans. In Burnett, W.C., and Riggs, S.R. (Eds.), *Phosphate Deposits of the World: Neogene to Modern Phosphorites*: Cambridge (Cambridge Univ. Press), 241–259.
- Schnitker, D., 1980. North Atlantic oceanography as possible cause of Antarctic glaciation and eutrophication. *Nature*, 284:615–616.
- Shackleton, N.J., and Hall, M.A., 1984. Carbon isotope data from Leg 74 sediments. In Moore, T.C., Jr., Rabinowitz, P.D., et al., *Init. Repts. DSDP*, 74: Washington (U.S. Govt. Printing Office), 613–619.
- Shackleton, N.J., Hall, M.A., Pate, D., Meynadier, L., and Valet, J.-P., 1993. High resolution stable isotope stratigraphy from bulk sediment. *Paleoceanography*, 8:141–148.
- Shackleton, N.J., and Kennett, J.P., 1975. Paleotemperature history of the Cenozoic and the initiation of Antarctic glaciation: oxygen and carbon isotope analyses in DSDP Sites 277, 279, and 281. In Kennett, J.P., Houtz, R.E., et al., *Init. Repts. DSDP*, 29: Washington (U.S. Govt. Printing Office), 743–755.
- Sigurdsson, H., Leckie, R.M., Acton, G.D., et al., 1997. *Proc. ODP, Init. Repts.*, 165: College Station, TX (Ocean Drilling Program).
- Vincent, E., and Berger, W.H., 1985. Carbon dioxide and polar cooling in the Miocene: the Monterey Hypothesis. In Sundquist, E.T., and Broecker, W.S. (Eds.), *The Carbon Cycle and Atmospheric CO_2 : Natural Variations Archaean to Present*. Geophys. Monogr., Am. Geophys. Union, 32:455–468.
- Woodruff, F., and Savin, S.M., 1989. Miocene deepwater oceanography. *Paleoceanography*, 4:87–140.
- , 1991. Mid-Miocene isotope stratigraphy in the deep-sea: high resolution correlations, paleoclimatic cycles, and sediment preservation. *Paleoceanography*, 6:755–806.

- Woodruff, F., Savin, S.M., and Douglas, R.G., 1981. Miocene stable isotope record: a detailed deep Pacific Ocean study and its paleoclimatic implications. *Science*, 212:665–668.
- Wright, J.D., and Miller, K.G., 1993. Southern Ocean influences on late Eocene to Miocene deepwater circulation. *Antarct. Res. Ser.*, 60:1–25.
- Wright, J.D., Miller, K.G., and Fairbanks, R.G., 1992. Early and middle Miocene stable isotopes: implications for deepwater circulation and climate. *Paleoceanography*, 7:357–389.
- Zachos, J.C., Flower, B., and Paul, H., 1997. Orbitally paced climate oscillations across the Oligocene/Miocene boundary. *Nature*, 388:567–570.

Date of initial receipt: 23 June 1998

Date of acceptance: 21 May 1999

Ms 165SR-016